EARTH SURFACE PROCESSES AND LANDFORMS
Earth Surf. Process. Landforms **36**, 334–346 (2011)

Published online 22 June 2010 in Wiley Online Library
(wileyonlinelibrary.com) DOI: 10.1002/esp.2041

Patterns of grain-size dependent sediment transport in low-ordered, ephemeral channels

Brendan T. Yuill[1] and Mary H. Nichols[2]
[1] Pontchartrain Institute for Environmental Studies, University of New Orleans, New Orleans, LA, USA
[2] Southwest Watershed Research Center, Agricultural Research Service, US Department of Agriculture, Tucson, AZ, USA

Received 4 December 2009; Revised 12 April 2010; Accepted 19 April 2010

*Correspondence to: Brendan T. Yuill, Pontchartrain Institute for Environmental Studies, University of New Orleans, New Orleans, LA 70148, USA.
E-mail: byuill@uno.edu

ESPL
Earth Surface Processes and Landforms

ABTRACT: Sediment data were analyzed to determine grain-size dependant factors affecting sediment transport in a low-ordered, ephemeral watershed. Sediment and flow samples were collected during 22 flow events at the outlet of a 4·53 ha sub-watershed within the Walnut Gulch Experimental Watershed in south-eastern Arizona. Measured concentrations ranged from 4191 to 115 045 mg l^{-1} and included grain sizes up to 8·0 mm in diameter. Two grain-size dependent transport patterns were observed, that of the finer grain-size fraction (approximately < 0·25 mm) and that of a coarser grain-size fraction (approximately ≥ 0·25 mm). The concentration of the fine fraction decreased with flow duration, peaking near the beginning of a flow event and declining thereafter. The concentration of the fine fraction showed slight trends with season and recovery period. The concentration of the coarse fraction displayed a slight negative trend with instantaneous discharge and was not correlated with event duration. These patterns typically produced a condition where the majority of the fine fraction of the sediment yield was evacuated out of the watershed before the hydrograph peak while the majority of the coarser sediment was evacuated during the falling limb of the hydrograph. Each grain-size dependent transport pattern was likely influenced by the source of the associated sediment. At the flow event time scale, the fines were primarily wash load, supplied from the hillslopes and the coarser grains were entrained from the channel bed. Because transport patterns differ based on grain size, attempts to define the total sediment concentration and sediment yield by the behavior of a single grain-size fraction may lead to erroneous results, especially when a large range of sediment grain sizes are present. Copyright © 2010 John Wiley & Sons, Ltd.

KEYWORDS: sediment transport; ephemeral flow, wash load, suspended sediment; semi-arid

Introduction

The magnitude of the sediment load transported within a river channel is influenced by the size of the sediments available for transport (Komar, 1987; Lisle, 1995). Different grain sizes are typically transported at different rates (Walling and Moorehead, 1987; Parker, 1990; Wilcock and McArdell, 1993; Andrews, 2000). Under most flow conditions, smaller grains are transported more readily than those larger. Also, different sediment grain sizes may be supplied to the channelized flow at different rates (Leopold *et al.*, 1964; Malmon *et al.*, 2004). Over short-time scales, the large sediment grains, such as sands, gravels, and cobbles, transported in river channels are supplied by the channel bed (Lisle, 1995; Church, 2006). The amount of each grain size located within the channel bed and its exposure to the tractive forces of the flowing water influences the rate at which that grain size can be entrained and transported downstream. Finer grains, such as that comprising the wash load, are primarily supplied to the river channel in runoff traveling as overland flow (Lekach and Schick, 1982; Walling and Moorehead, 1987). The rate that overland flow transports sediment to a river channel is controlled by the flow hydraulics, the amount of the entrainable sediment located on the hillslopes, and the hillslope physiography which includes factors such as lithology, relief, vegetation, and micro-topography (Komar, 1980; Lekach and Schick, 1982; Walling and Webb, 1982; Syvitski *et al.*, 2000; Malmon *et al.*, 2004). Because sediment transport rates vary with grain size, there are few instances where a specific discharge will produce similar rates of transport for each grain size present.

Fluvial sediment transport studies often report the total transport rate occurring within a channel reach rather than that of specific grain-size fractions. However, different sediment grain sizes have variable importance to sedimentation management and engineering projects (Morris *et al.*, 2008; Shields *et al.*, 2008). For example, fine grains typically have greater impact on water quality while coarser grains typically have greater impact on channel stability (Novotny, 1980; Leopold, 1992; Stone and Walling, 1997). Thus for many sedimentation engineering or management projects, it is more important to understand the transport patterns of specific grain sizes rather than that of the total sediment load (Walling and Moorehead, 1987). If the transport patterns of all grains are assumed to be similar to the total rate and they are not, the projects may be subject to failure. Therefore, it is important that we understand the manner in which different grain sizes are transported in natural fluvial systems; if they have unique transport patterns, if their transport patterns are different than that of the total load, and if their transport patterns are of a significant scale to affect potential engineering and management projects.

This study investigates grain-size selective transport patterns in an alluvial, headwater watershed with an ephemeral flow regime. This environment is uniquely suited to study how grain-size may affect transport because ephemeral channels often have poorly sorted beds with a large range of grain sizes available for transport (Laronne *et al.*, 1994; Andrews, 2000; Powell *et al.*, 2001). Further, it is easier to constrain the source of wash load in headwater watersheds because of the absence of tributary inputs, making it more likely that the wash load originated within the proximal watershed hillslopes.

The objectives of this study are (1) to identify if the concentration of transported sediment exhibit grain-size selective transport patterns, (2) to quantify how the grain-size selective transport patterns, if present, are different from the mean pattern of the total sediment load and from one another, (3) to explore the dependency of grain-size selective transport patterns on metrics of flow strength, duration, and sediment source, and (4) to determine if the grain-size selective transport patterns significantly affect watershed sediment delivery.

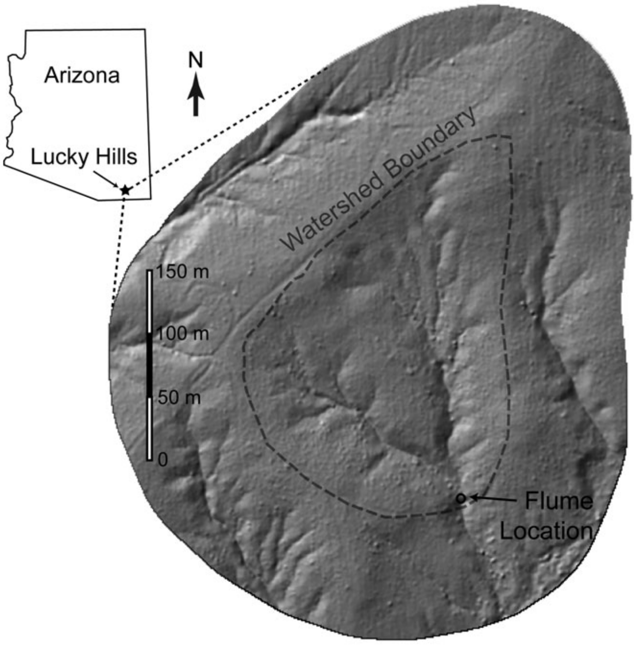

Figure 1. Hillshade map of the Lucky Hills 104 field site.

Study Site

Walnut Gulch experimental watershed (WGEW)

The 150 km^2 USDA-ARS Walnut Gulch experimental watershed (WGEW) (Renard *et al.*, 2008; http://tucson.ars.ag.gov) in south-eastern Arizona is an ephemeral tributary to the San Pedro River. The watershed is defined by basin and range physiography, with elevations ranging from 1800 m at its headwaters in the Dragoon Mountains to 1200 m at its outlet. Average monthly temperatures range from 22°C in January to 33°C in July. Mean annual precipitation for the entire watershed is approximately 350 mm, with the majority occurring during the summer monsoon season (July–September) (Nichols *et al.*, 2002). Almost all runoff is generated during the summer monsoon season. The western two-thirds of the watershed are shrubland and the eastern third is primarily grassland.

Lucky Hills 104 sub-watershed

The 4·53 ha (45,300 m^2) Lucky Hills 104 watershed (Figure 1) is a low-order, unit-source watershed located in the north central region of Walnut Gulch watershed. The watershed hillslopes are covered by an array of drought resistant shrubs, including creosote bush (Larrea tridentata [DC.] Cov.), acacia (Acacia constricta Benth.), and tarbush (Flourensia cernua DC.) Between 1963 and 2007, the mean annual precipitation measured locally at Lucky Hills was 295 mm with a standard deviation of 80 mm.

The Lucky Hills 104 watershed exhibits an ephemeral flow regime. Flow hydrographs have steep rising limbs, generally peaking during the first third of the event's duration. The receding limbs are more gradual than the rising limbs but are still sharper than those of floods in more humid regions. Hydrographs commonly contain a single peak; however, flow events with relatively long durations occasionally exhibit multiple peaks. The majority of flow events last less than one hour, although flows lasting over six hours have been recorded. The small size of the watershed produces a short time of concentration for flow events, on the order of tens of minutes. On average, five flow events occur annually but it is not atypical for a year to pass without any flows.

The mean channel gradient in Lucky Hills is 0·027 m m^{-1}. The channel width ranges from 0·5 to 2·0 m. The bank heights range from a few centimeters with low bank slopes to 1·0 m with near vertical, incised banks. The channel bed within Lucky Hills varies from local areas of cobbles to fine sand and exhibits patchiness resulting from hydraulic sorting and spatial differences in hillslope sediment delivery (Yuill *et al.*, 2010).

Methodology

Runoff and sediment measurement

Runoff and sediment transport were measured at the outlet of the Lucky Hills 104 watershed. Channelized runoff was measured using a calibrated, Santa-Rita type supercritical flume. The flume accelerates flow velocity to prevent sediment deposition within its channel. During flow events, the flume automatically records flow stage at 15 second intervals using an integrated silling well and float system (Smith *et al.*, 1981).

Flow was sampled while passing through the flume by an automated traversing-slot sampler to compute fluvial sediment concentration (Renard *et al.*, 1986, Nichols *et al.*, 2008). The traversing-slot sampler takes a total load, depth integrated sample along the wetted width of the flume. The slot sampler initially samples at three minute intervals until 15 minutes had elapsed and then switches to a five minute sample interval for an addition 15 minutes. If flow continues beyond 30 minutes, the sampler switches to a 10 minute interval for the duration of the flow. The sampler inlet is 13 mm wide. In practice, the sampler is assumed to reliably retain grains 8 mm (grain sizes are reported in terms of the intermediate diameter of the grain) and finer; however, larger grain sizes are occasionally observed in the sampled sediment (Nichols *et al.*, 2008).

Table I. Categorization of sediment by transport mechanism, source, and Rouse number

Sediment category	Transport mechanism	Morphological source	Rouse number range
Wash load	Suspension (unstratified in flow)	Hillslopes	<0·8
Suspended sediment	Suspension (stratified in flow), saltation	Channel bed	0·8–2·6
Bed load	Traction (rolling, sliding, bouncing)	Channel bed	>2·6

Note: Rouse number threshold values are a synthesis of those reported in the literature (e.g. Julien, 1998; Raudkivi, 1998). Based on Church (2006), Figure 1.

The traversing arm of the sampler rests in an out-of-flow position. At a prescribed flow depth threshold the arm becomes activated, sampling at the set intervals until flow once again descends below the depth threshold. Once activated, the sampling arm traverses the width of the flow at a uniform velocity set to capture a minimum 1 l volume of flow. If a single traverse is inadequate to capture a 1 l sample, a weight gauge under the sample bottle will trigger an additional traverse. The sampler is gauged to only sample the flume width experiencing flow at the time of measurement. Each sample is stored in one of 20 plastic 2 l bottles placed within a vertically oriented, weight driven wheel. The rotating wheel is housed adjacent to the flume, excavated into the channel bank in a manner not to affect channel morphology or store runoff. After each sampler traverse, the wheel holding the sample bottles rotates to an intermediate position with no bottle present in the sampling position to prevent contamination. The next empty sample bottle is rotated into the sampling position immediately preceding the initiation of a sampling sequence. The sampler is powered by a solar generator connected to two 12-V d.c. motors, one attached to the sampling arm and the other to the rotating table. Experimental calibration tests using flow with known sediment concentrations found the sampler to perform as well or better than other typical sediment sampling methods (i.e. US D-48 dip sampler) (Renard *et al.*, 1986).

The samples of flow and sediment were weighed to determine a wet-weight mass and then oven dried. Sediment concentration was computed from the wet and dry-weight mass and converted into milligrams per liter (mg l^{-1}) units. Dry samples were sieved by a mechanical shaker to determine grain-size distribution (GSD). The GSDs are classified using the standard phi intervals; 4·0–8·0 mm (although this interval may contain larger grain sizes due to the constraints of sampling method as mentioned earlier), 2–4 mm, 1–2 mm, 0·5–1 mm, 0·25–0·5 mm, 0·125–0·25 mm, 0·063–0·125 mm, and <0·063 mm.

Sediment flux (in kg s^{-1}) was approximated from the concentration values by multiplying the concentration (in mg l^{-1}) by the corresponding discharge (in l s^{-1}). Event sedigraphs were extrapolated from measured runoff and sediment concentration values using standard procedures of integration (e.g. Porterfield, 1972). For a description of the procedure and assumptions of computing sediment yields in this manner see Nearing *et al.* (2007).

Channel bed grain size measurement

Bulk samples of channel bed sediment were collected and sieved to determine the surface and subsurface GSD at 12 monumented cross-sections located along the channel network. Separate surface and subsurface samples were taken at each cross-section. Subsurface samples were taken below the depth of the largest surface grain diameter present. At each sampled location, the bed material collected spanned the channel width. The composite bulk sample size (36 kg) was below that recommended by Church *et al.* (1987) to ensure an un-biased estimated GSD value but it was approximate to the 'practical' sample size recommended by Wentworth (1926) (i.e. 32 kg).

For the purposes of this study, a modified GSD was computed using a truncated version of the full bed GSD. The modified GSD only considered grain sizes measurable by the traversing-slot sampler, i.e. that less than 8·0 mm.

Estimation of transported sediment properties and flow hydraulics

Transported sediment was classified into three categories (wash load, suspended sediment, and bedload) based on the computed Rouse numbers for each grain-size fraction (Table I). The wash load is composed of highly mobile sediment that is typically not prone to deposition while entrained by flow and is therefore not found within the channel bed material at the same abundance as the sediment in the other categories (Komar, 1980; Church, 2006). Suspended sediment is composed of suspended or saltating bed material and bedload is composed of bed material transported along the surface of the channel bed by the tractive forces of flow.

The Rouse number (P) was computed as

$$P = \frac{\omega_s}{\kappa u_*}$$

where ω_s is the settling velocity, κ is von Karman's constant (0·41), and u^* is the instantaneous shear velocity of the flow. Settling velocity is dependent on grain size and was calculated using the method developed by Dietrich (1982). Shear velocity was estimated as the square root of the instantaneous boundary shear stress (τ) over the density of water (ρ). Boundary shear stress is approximated as $\tau = \rho gRS$, where g is acceleration due to gravity (9·81 m s^{-2}), R is the mean hydraulic radius of the channel, and S is the mean longitudinal channel slope. This derivation of boundary shear stress is an approximation of the fluid stress borne by the bed grains and while commonly employed in a wide range of geomorphic studies (e.g. Batalla and Martin-Vide, 2001; Habersack and Laronne, 2001; Tucker *et al.*, 2006; Powell *et al.*, 2007), it uses assumptions (e.g. steady, uniform flow) that are often violated in natural flows. Hydraulic radius was computed for 20 cross-sections within the lower channel system for the range of observed flows. Computed values were used to derive an average discharge-hydraulic radius relationship. The flow area and wetted perimeter were determined by routing the flow discharge through the channel network using the resistance equation of Hey (1979),

$$\frac{U}{(gRS)^{0.5}} = 5.62 \log\left(\frac{aR}{3.5D_{84}}\right)$$

where U is mean flow velocity, D_{84} is grain size in which 84% of the channel bed grains are finer. The variable a is a channel shape factor defined as

$$a = 11{\cdot}1\left(\frac{R}{D_{max}}\right)^{-0{\cdot}314}$$

where D_{max} is thalweg depth. This resistance equation was selected because the required input parameters of bed texture and channel geometry are known at this field site and because of its applicability to low-order channels without the presence of large roughness elements (i.e. boulders) (Thorne *et al.*, 1985). The resistance equation predictions were validated against high water marks measured after the conclusion of multiple flow events.

Data analysis

Regression analyses were used to verify observed trends in the sediment concentrations collected in transport. The strength of the observed trends was gauged by the coefficient of determination (r^2) value, where coefficients with p-values less than 0·01 were interpreted as significant for the purposes of this study. To determine the correlation between groups of values (such as the concentrations of each sediment grain size sampled at a specific time interval), Pearson product-moment correlation coefficients were computed. Correlation coefficients range between 1·0 and –1·0 with higher absolute values indicating greater correlation. Negative values indicate the correlation is negative.

Results

Runoff

From 1998 through 2007, 64 runoff events were recorded at the watershed outlet. The mean flow volume was 101·1 m^3 and the mean peak discharge was 0·18 m^3 s^{-1}. The maximum recorded peak discharge for the study period was 0·66 m^3 s^{-1}, measured during a flow with a volume of 451·0 m^3. Using the historical flow data dating to 1963 (http://www.tucson.ars.ag.gov/dap), the calculated peak discharges for the flow events with two, 10, and 50 year reoccurrence intervals are 0·35 m^3 s^{-1},0·86 m^3 s^{-1}, and 1·27 m^3 s^{-1}, respectively, based on a Log-Pearson Type III distribution.

Sediment transport concentrations

During the study period 1998–2007, 83 sediment samples were collected from 22 runoff events and analyzed for sediment transport concentration and grain-size distribution. Total sampled sediment concentrations ranged from 4191 to 115 045 mg l^{-1}. The concentrations of the 83 sediment samples are displayed in Figure 2. The mean sediment concentration was lower after the hydrograph peak than before it, although the difference in value was not statistically significant (Table II). The sediment concentrations display a weak negative trend with instantaneous discharge (r^2 = 0·08, p-value < 0·01).

Grain-size properties of the sediment in transport

The mean channel bed GSD was 'very poorly sorted' (Folk and Ward, 1957) with a median grain size (D_{50}) of 2·83 mm (Figure 3). For the majority of the channel bed, there were no observable textural differences between the surface and subsurface bed material. The surface of the channel bed contained sporadic patches (~ 0·25–2·0 m^2 in area) of relatively coarse grains (i.e. gravel and cobble) that did not typically extend into the subsurface, which caused the bed surface to be coarser than the subsurface locally.

The mean GSD of the sediment measured in transport was finer than the GSD of the channel bed material (Figure 4A). The D_{50} of the sediment sampled in flow was 0·56 mm while that measured from the channel bed material GSD truncated at the maximum grain size measurable by the traversing-slot sampler was 1·13 mm. On average, a much larger fraction of

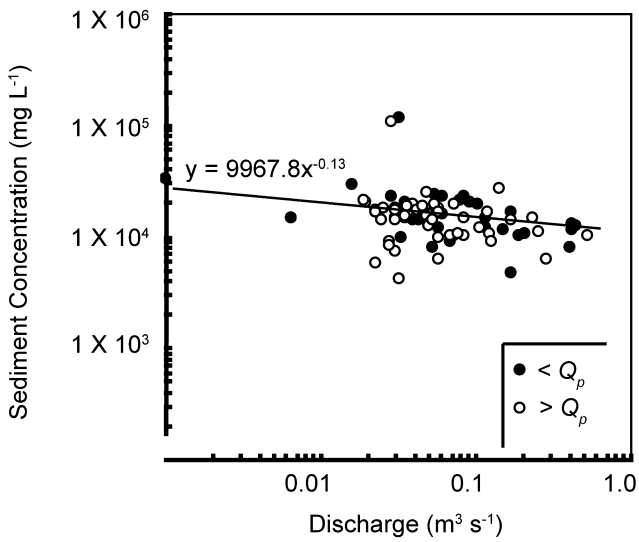

Figure 2. Total sediment concentrations collected at the watershed outlet plotted against the instantaneous discharge at the time of sampling. Measurements collected before the hydrograph peak (<Q_P) and afterwards (>Q_P) are differentiated.

Table II. Summary sediment concentration values differentiated by metrics of time and discharge

	Total concentration (mg l^{-1})		Fine concentration (mg l^{-1})		Coarse concentration (mg l^{-1})	
Subset	Mean	Standard deviation	Mean	Standard deviation	Mean	Standard deviation
All samples	17209	15871	4616	3037	12593	14486
<Q_p	18476	17639	*6261*	3255	12215	16000
>Q_p	16404	16237	*3494*	3355	12910	12882
Q_1	20424	21586	4177	3491	16247	19449
Q_2	13875	5037	5076	2360	8799	4413

Note: <Q_p = measured before the hydrograph peak, >Q_p = measured after the hydrograph peak, Q_1 = measured during the lowest half of discharge values, Q_2 = measured during the highest half of discharge values. Proximal italic values were determined to be significantly different (p-value < 0·01) by a modified Student's T-test (i.e. Welch's T- test).

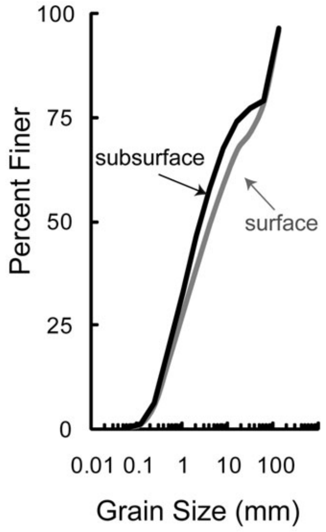

Figure 3. The averaged surface and subsurface grain-size distributions of the channel bed material.

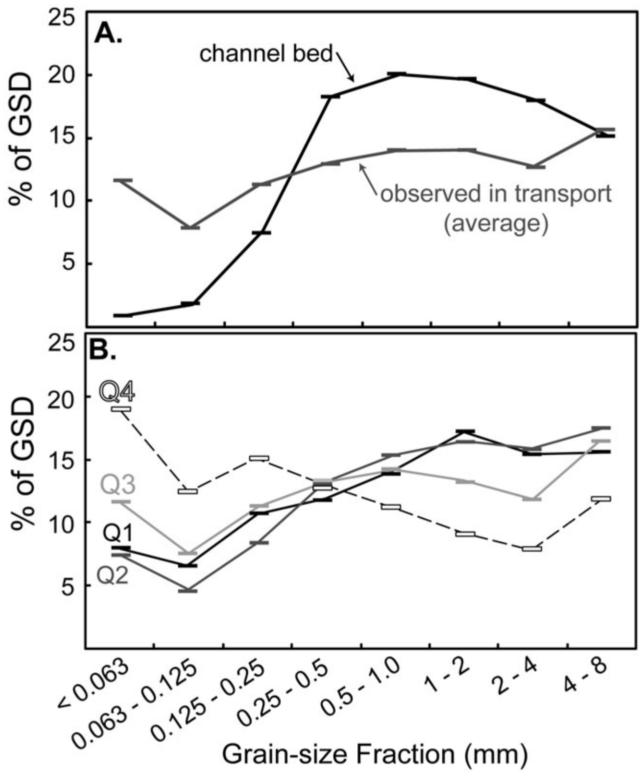

Figure 4. (A) The grain-size distribution (GSD) of the channel bed (composite of both surface and subsurface samples) truncated at 8·0 mm and the mean GSD for the sediment sampled in flow. (B) The mean GSD for sediment transport sampled in four ranges of discharge (approximate to quartiles), Q1 (0·001–0·03 $m^3 s^{-1}$), Q2 (0·03–0·05 $m^3 s^{-1}$), Q3 (0·05–0·1 $m^3 s^{-1}$), and Q4 (0·1–0·53 $m^3 s^{-1}$).

the sediment sampled in transport was composed of grain sizes <0·25 mm (31%) than that located in the truncated channel bed GSD (10%). The size of the fraction of the sediment in transport composed of these finer grain sizes typically increased with discharge (Figure 4B).

Observation of the GSD of the sampled sediment concentrations showed that finer grain sizes tended to exhibit different transport patterns than the coarser grains during flow events (Figure 5). Table III shows a matrix of correlation coefficients computed for the relationship between the concentrations of each individual grain-size fraction analyzed from the 83 sediment samples. Correlation coefficients greater than 0·29 are statistically significant at 99% confidence (df = 81). Correlation gradually decreased as the magnitude of the difference in grain size increased. Analysis of the correlation coefficients of the coarser grain sizes, which composed the majority of the truncated channel bed GSD (i.e. 0·25–0·5 mm, 0·5–1·0 mm, 1–2 mm, 2–4 mm, and 4–8 mm), found that these grain sizes tended to behave similarly. When grouped into a comprehensive 'coarse grain-size fraction (i.e. grains ≥ 0·25 mm)', the mean correlation coefficient between group members is 0·74. The finer grain sizes, which were not found in abundance within the channel bed GSD (i.e. that <0·063 mm, 0·063–0·125 mm, and 0·125–0·25 mm), also tended to behave similarly. When grouped into a 'fine grain-size fraction (i.e. <0·25 mm)', the mean correlation coefficient between group members is 0·69. The mean (of the absolute value) of the correlation coefficients calculated between the members of the fine and the coarse grain-size fractions is 0·21.

The correlation matrix indicates that the concentrations of the coarser grain sizes are better correlated to the total sediment concentration than the finer grain sizes. The slope of the linear relationship between the total concentration and the concentration of the coarse grain-size fraction is 0·90 (r^2 = 0·97), indicating that increases in total sediment concentration were predominately a result of increased coarse sediment (Figure 6). The linear relationship between the total concentration and the concentration of the fine grain-size fraction displays considerably more variability (r^2 = 0·28) than that between the total and coarse sediment concentrations.

Figure 7 shows the sediment concentrations plotted against flow discharge as differentiated between the fine and coarse grain-size fractions. The data are summarized in Table II alongside summary data for the total sediment concentration. The concentration of the fine grain-size fraction shows a strong tendency to be greater before the hydrograph peak than afterwards. Unlike the total sediment concentration, the fine grain-size fraction displays no trend with discharge. In contrast, the coarse grain-size concentrations display a statistically significant tendency to decrease with increasing discharge (r^2 = 0·15, p-value < 0·01) and show little difference before and after the hydrograph peak.

Temporal patterns of sediment transport by grain-size fraction

To better illustrate the temporal patterns in the sediment concentration data, both the fine and coarse grain-size fractions are plotted by event duration in Figure 8. The concentration of the fine grain-size fraction is significantly correlated to the elapsed time of the event, highest at the beginning of the event and typically declining thereafter. Figure 8(A) displays that the temporal trend in the fine grain-size fraction can be similarly described as linear (r^2 = 0·19, p-value < 0·01) or logarithmic (r^2 = 0·21, p-value < 0·01). In Figure 8, the event duration has been standardized by the elapsed time of the hydrograph peak, which improves the ability to visually compare sediment trends in hydrographs of different lengths and improves the overall correlation between the concentration and duration values. As displayed in Figure 8(B), the concentration of the coarse grain-size fraction displays no significant correlation with event duration.

The concentration of the fine grain-size fraction also displays a slight seasonal trend, decreasing on average throughout the annual monsoon season. Figure 9 shows the fine sediment concentration by the day of the year in which it was

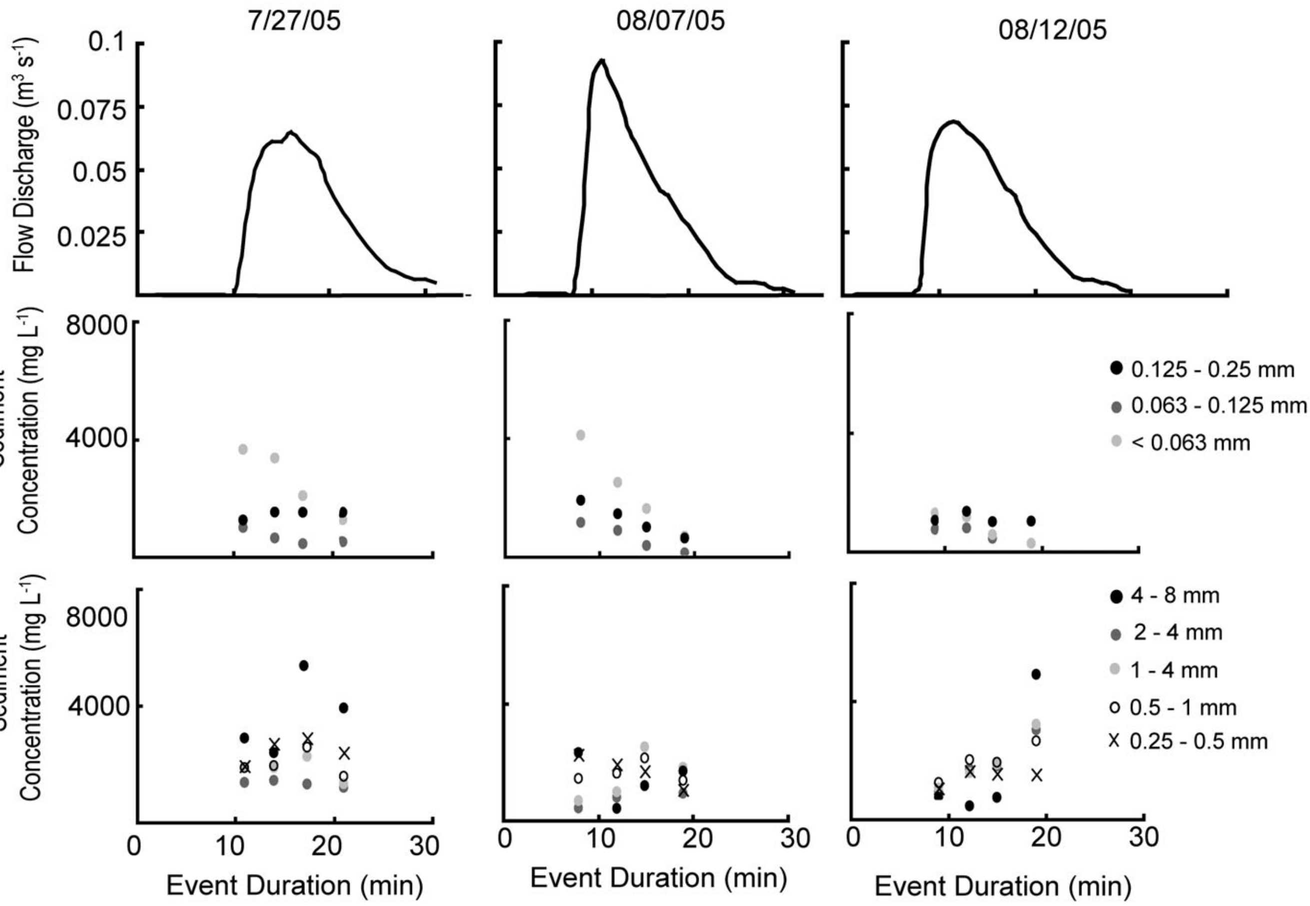

Figure 5. Flow and sediment concentration data for three consecutive flow events.

Table III. A correlation matrix computed for the measured sediment concentrations of each analyzed grain-size fraction and the total measured concentration (n = 83)

	Grain-size fraction (mm)							
Grain-size fraction (mm)	4–8	2–4	1–2	0·5–1	0·25– 0·5	0·125–0·25	0·063–0·125	<0·063
4–8	1·00							
2–4	0·71	1·00						
1–2	0·60	0·98	1·00					
0·5–1	0·67	0·96	0·97	1·00				
0·25–0·5	0·82	0·83	0·79	0·88	1·00			
0·125–0·25	0·61	0·52	0·47	0·52	0·72	1·00		
0·063–0·125	0·38	0·32	0·29	0·32	0·48	0·84	1·00	
<0·063	0·02	–0·04	–0·03	–0·01	0·13	0·45	0·75	1·00
Total concentration	0·86	0·93	0·89	0·92	0·93	0·73	0·54	0·16

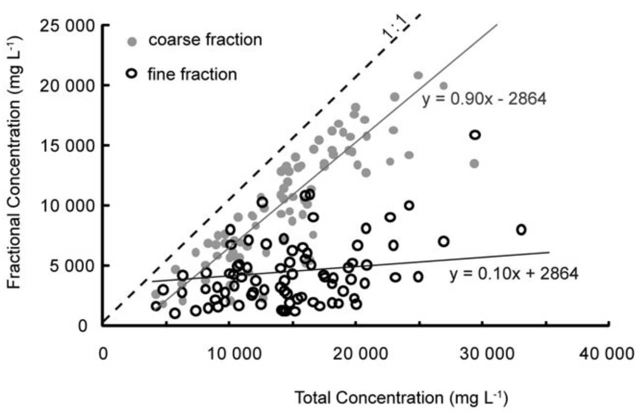

Figure 6. The sediment concentrations for the fine (<0·25 mm) and coarse (≥0·25–8·0 mm) grain-size fractions plotted against the total concentration of each sediment sample collected.

collected for the three consecutive years in which every flow event was sampled. The last two years (2006 and 2007) show a trend of decreasing fine sediment concentration values throughout the monsoon season. The first year (2005) displays this trend until the last flow event of the year (occurring on September 8) which produced relatively high sediment concentrations.

Patterns of sediment transport by sediment category

The grain sizes sampled by the traversing-slot sampler fall into three sediment categories, wash load, suspended sediment, and bedload. Grain sizes finer than 0·25 are categorized as wash load for the range of discharges in which sediment was sampled in this study (Figure 10). Coarser grains are

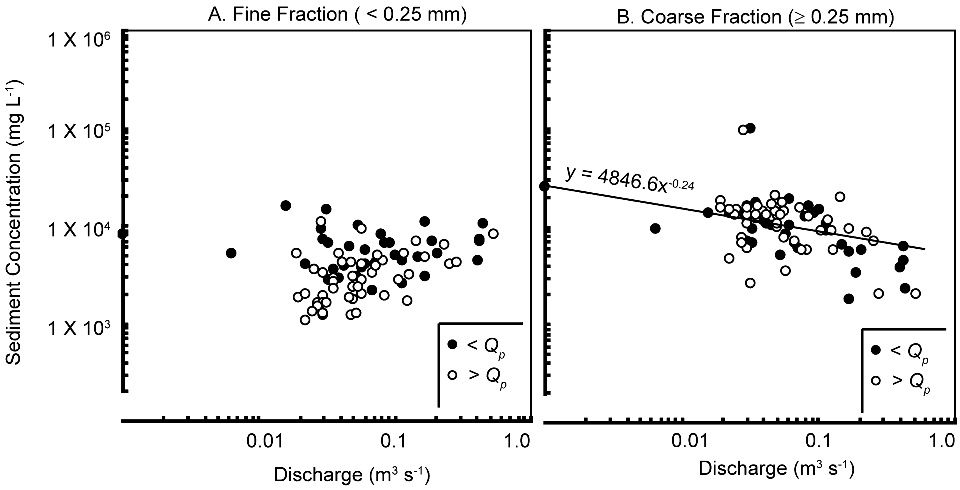

Figure 7. Sediment concentrations for the (A) fine and (B) coarse grain-size fractions plotted against the instantaneous discharge. Measurements collected before the hydrograph peak ($<Q_P$) and afterwards ($>Q_P$) are differentiated.

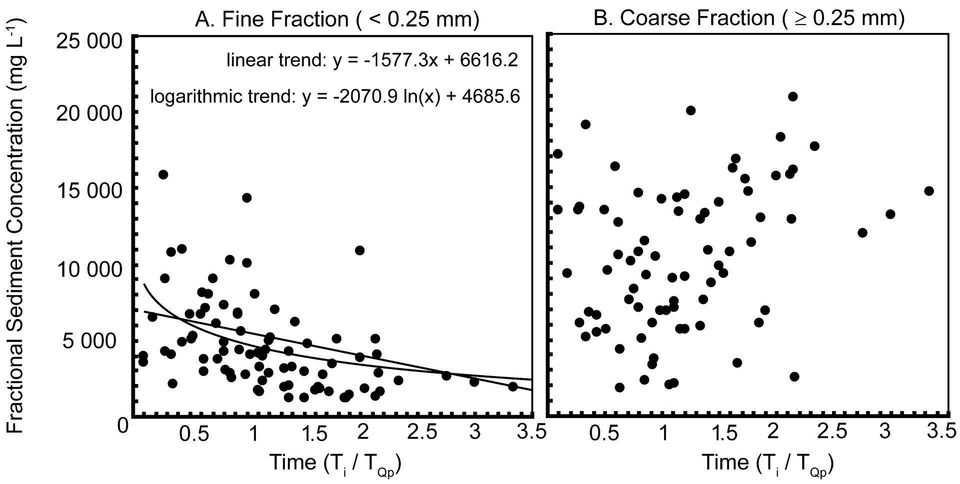

Figure 8. (A) Fine and (B) coarse sediment concentration plotted against event duration. Event duration was standardized by dividing the elapsed time from the start of the flow event and the time at which the sample was collected (T_i) by the elapsed time from the start of the flow event and the time of the hydrograph peak for the flow event it was sampled (T_{Qp}).

categorized as either suspended sediment or bedload with the categorization of grain sizes between 0·25 and 2·0 mm dependent on flow discharge.

Observations indicate that the fraction of the sampled sediment concentrations composed of wash load increased with discharge (Figure 11). The fraction of sediment transport composed of wash load increased from an average of 30% at the lowest sampled discharges to exceeding 75% at the highest sampled discharges. As the discharge approached 0·4 $m^3 s^{-1}$, nearly all of the sampled sediment was categorized as wash load or suspended sediment.

Sediment flux

While sediment traveling in suspension is typically examined in terms of concentration, bedload is more commonly described in terms of mass flux. Table IV displays the power-law relationship for the computed sediment flux of each individual coarse grain-size fraction and excess Shields stress. Excess Shields stress ($\tau^* - \tau^*_c$) is a dimensionless metric of the fluid forces borne by a sediment grain (τ^*) beyond that required for initial grain entrainment (τ^*_c). Shields stress (τ^*) equals

$$\tau^* = \frac{\tau}{(\rho_S - \rho) g D}$$

where ρ_s is density of sediment and D is grain diameter. The critical Shields stress (τ^*_c) ranges between 0·03 and 0·06 for typical natural river beds and the averaged value (0·045) is assumed for this study (Church, 2006). Study results show that the exponents of the power laws systematically decrease with increasing grain size, ranging from approximately 1·1 to 2·5. The power-law relationship between the flux of the full coarse grain-size fraction (0·25–8·0 mm) and shear stress (τ) (r^2 = 0·65, p-value < 0·01) is shown in Figure 12.

Watershed sediment yield

Figure 13 illustrates the calculated hydrograph and sediment yield for the first flow of 2005. The majority of the fine grain-size sediment delivery occurred during the rising limb of the flow hydrograph while the majority of the coarse sediment delivery and flow discharge occurred during the falling limb. These trends in sediment delivery were found during most

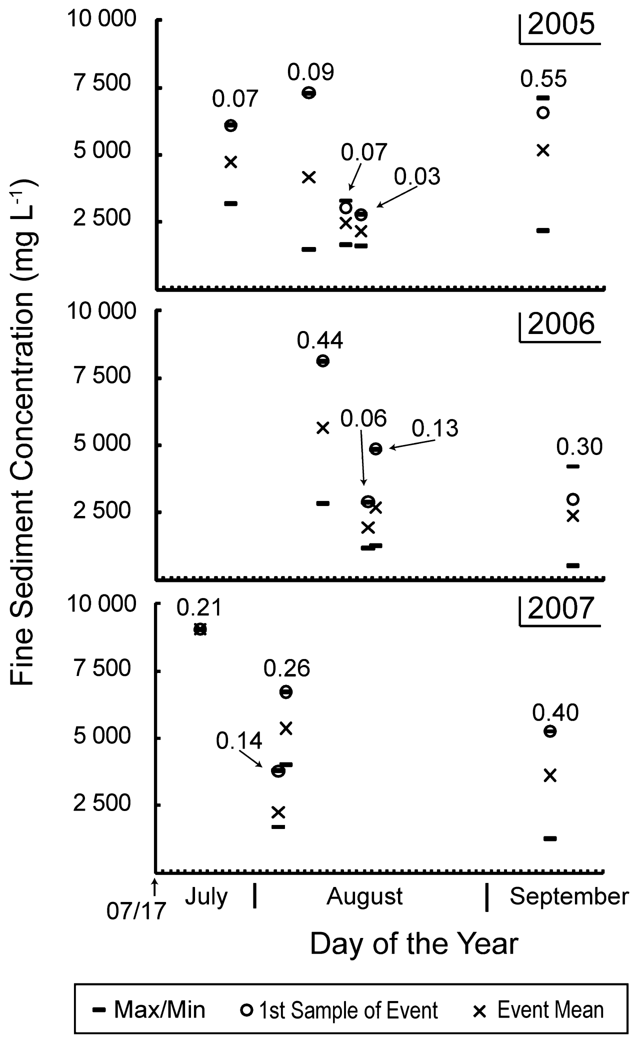

Figure 9. Fine sediment concentration (<0·25 mm) plotted versus the day of the year in which the sample was collected. The maximum, mean, minimum, and first sample collected values for each flow event are displayed. The numerical values near each group of concentration values define the peak flow (in m^3 s^{-1}) for each flow event.

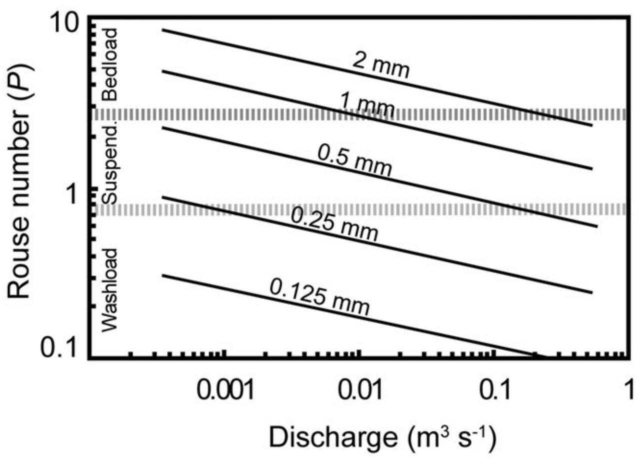

Figure 10. The categorization of five grain sizes into wash load, suspended sediment, or bed load by flow discharge. Categorization is based on the computed Rouse number for each grain size.

flows. Table V lists the values of flow volume and sediment yield leaving the watershed outlet during the rising and falling limbs of the hydrograph for flows occurring from 2005 through 2007, which are the years in which every flow was success-

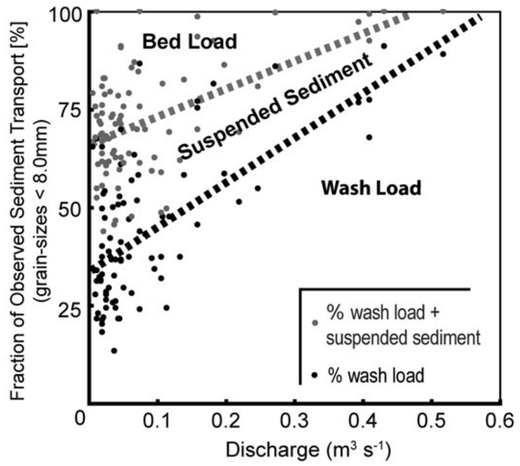

Figure 11. The fraction of the sampled sediment concentrations categorized as wash load, suspended sediment, and bed load by flow discharge. Categorization was based on the computed Rouse number for each grain-size fraction (as observed in Figure 10). The black trend line is fit to the wash load data series and the gray trend lines is fit to the wash load + suspended sediment data series. Both trend lines are statistically significant (p-value < 0·01).

fully sampled. Over this time period, 56% of the fine sediment yield, 38% of the coarse sediment yield, and 46% of the total flow volume was evacuated out of the watershed before the hydrograph peak of each flow event.

Discussion

Sediment transport in Lucky Hills 104

The total sediment concentrations measured at the outlet of Lucky Hills 104 were relatively high compared to that found in most perennial fluvial systems but were comparable to that reported in other studies in ephemeral watersheds (e.g. Frostick *et al.*, 1983; Alexandrov *et al.*, 2003; Malmon *et al.*, 2004; Cohen and Laronne, 2005; Malmon *et al.*, 2007; Leopold *et al.*, 1964; Milliman and Meade, 1983; Syvitski *et al.*, 2000). Sediment samples collected during this study with the traversing-slot sampler were composed of a wider range of grain sizes than that typically reported in studies of sediment transport, which constrain the range of grain sizes measured by transport mode (i.e. that traveling in suspension or bedload). The methodology used in this study ensures that the same particular grain-size fraction (≤8·0 mm) was equitably sampled, independent of the transport mode in which the grains were traveling. While the relatively high sediment concentrations reported in this study may have been influenced by the fact that they were derived from sediment traveling by more than one mode, calculations show that the majority of the grains were traveling in suspension, as either wash load or suspended sediment, for the range of discharges from which sediment was sampled.

The total sediment concentration displayed a weak negative trend with discharge. Sediment transport studies in other fluvial systems have observed variable dependence of sediment concentration on flow discharge (Renard and Laursen, 1975; Dunkerley and Brown, 1999; Syvitski *et al.*, 2000; Malmon *et al.*, 2004; Cohen and Laronne, 2005; Alexandrov *et al.*, 2006). Typically, the relationship is reported as a positive power law; however, there is no consensus on the controlling influences of the power-law coefficients, which have been correlated to a range of variables including basin physiography, climate, and sediment supply in past studies.

Table IV. Calculated sediment flux power laws for the coarse grain-size fractions

Grain-size fraction (mm)	Sediment flux power law	
4–8	$Q_S = 0{\cdot}325(\tau^* - \tau_c^*)^{1{\cdot}10}$	$r^2 = 0{\cdot}16$, p-value < 0·01
2–4	$Q_S = 0{\cdot}167(\tau^* - \tau_c^*)^{1{\cdot}42}$	$r^2 = 0{\cdot}34$, p-value < 0·01
1–2	$Q_S = 0{\cdot}062(\tau^* - \tau_c^*)^{1{\cdot}89}$	$r^2 = 0{\cdot}54$, p-value < 0·01
0·5–1·0	$Q_S = 0{\cdot}012(\tau^* - \tau_c^*)^{2{\cdot}24}$	$r^2 = 0{\cdot}78$, p-value < 0·01
0·25–0·5	$Q_S = 0{\cdot}002(\tau^* - \tau_c^*)^{2{\cdot}49}$	$r^2 = 0{\cdot}83$, p-value < 0·01

Note: Q_S = sediment flux (in kg s^{-1} m^{-1}); τ^* = Shields stress; τ_c^* = critical Shields stress (approximated as 0·045).

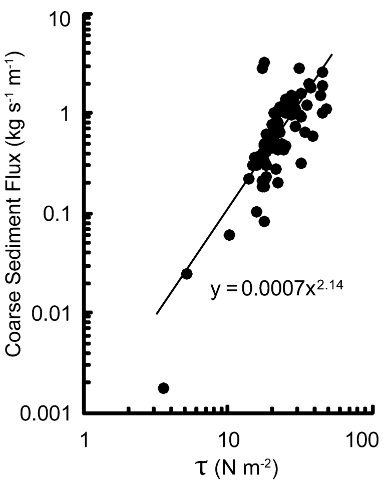

Figure 12. The flux of the coarse sediment fraction plotted against calculated reach-averaged shear stress.

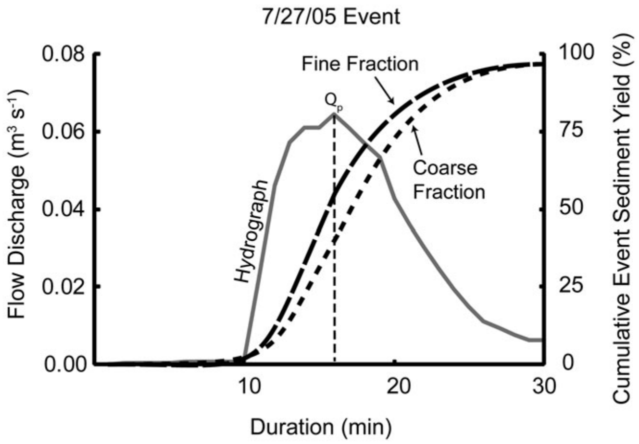

Figure 13. Flow discharge and cumulative sediment yields for the July 27, 2005 (7/27/05) flow event.

Table V. Calculated flow volume and sediment yield for four individual flow events in 2005 and for the total values estimated for 2006 and 2007

	Discharge		Fine yield		Coarse yield	
Flow date	$<Q_p$ (m^3)	$>Q_p$ (m^3)	$<Q_p$ (kg)	$>Q_p$ (kg)	$<Q_p$ (kg)	$>Q_p$ (kg)
7/27/2005	19·0 (44%)	24·5 (56%)	108 (55%)	88 (45%)	196 (39%)	309 (61%)
8/7/2005	12·6 (27%)	33·6 (73%)	79 (41%)	113 (59%)	81 (25%)	248 (75%)
8/12/2005	15·6 (35%)	28·7 (65%)	51 (46%)	58 (54%)	104 (25%)	313 (75%)
9/8/2005	297·6 (59%)	208·8 (41%)	1887 (62%)	1135 (38%)	1373 (44%)	1766 (56%)
2006 events n = 4	131·4 (39%)	208·8 (61%)	703 (49%)	721 (51%)	951 (37%)	1592 (63%)
2007 events n = 3	126·3 (37%)	216·8 (63%)	563 (51%)	547 (49%)	1072 (36%)	1900 (64%)
Total	602·5 (46%)	721·1 (54%)	3390 (56%)	2662 (44%)	3777 (38%)	6127 (62%)

Note: $<Q_p$ = occurring before the hydrograph peak; $>Q_p$ = occurring after the hydrograph peak.

Previous suspended sediment studies in ephemeral channels have found a relatively strong relationship between sediment concentrations and metrics of flow relative to that reported in perennial channels, attributing the strength of the relationship to the abundance of sediment typically stored in ephemeral watersheds (Leopold *et al.*, 1964; Reid and Frostick, 1987; Alexandrov *et al.*, 2003).

Grain-size dependent sediment transport patterns

The lack of a distinct transport trend observed in the total sediment concentration may be due to the fact that it was composed of a wide range of grain sizes that do not necessarily exhibit similar transport patterns. The finer grain sizes concentration were predominately correlated with event duration while the coarser grain sizes displayed a more coherent trend with flow discharge (and no trend with event duration).

We interpret that the fine grain-size fraction exhibited a different transport pattern than the coarser fraction because it was primarily composed of wash load sediment. Wash load travels in suspension, relatively unstratified throughout the flow column and travels at or near the velocity of the flowing water (Komar, 1980; Church, 2006). This categorization is based on the computed Rouse number for each grain-size fraction measured in transport and from examination of the grain-size distribution of the channel bed. In Lucky Hills, the fine grain-size fraction (<0·25 mm) comprised only 10% of the channel bed material that was measureable by the slot sampler (i.e. <8 mm) but constituted approximately 30 to 80% of the sediment measured in transport. This indicates that the channel bed material was not the primary source for the fine grain-size fraction sampled in transport. The coarser sediment was categorized as suspended sediment and bedload, which are composed of entrained bed material.

Patterns of the fine grain-size fraction

The concentration of the fine grain-size fraction declined in time, through each flow event and also seasonally, although to a lesser extent. Observations of waning sediment concentrations at the flow event time scale (which is often referred to as 'clock-wise hysteresis') have been commonly attributed to a relative time dependent decrease in sediment supply (e.g. Renard and Laursen, 1975; Wood, 1977; Lekach and Schick, 1982; Reid and Frostick, 1987; Dunkerley and Brown, 1999; Malmon *et al.*, 2004; Malmon *et al.*, 2007). This relative drop in supply has been explained by both a surge in the sediment supply during the initial onset of the flow and by the time dependent waning of hillslope sediment reserves. However, other sediment transport studies in ephemeral channels have related the time dependent decrease in sediment transport values to processes other than sediment supply, such as steep fluctuations in the flow's energy slope (e.g. Meirovich *et al.*, 1998) and high rates of transmission loss (e.g. Mudd, 2006).

Limited sediment supply may also influence the fine sediment concentrations at the seasonal and annual time scale (Walling and Webb, 1982). If the observed decline in sediment concentration during each flow event was due to depleting sediment supply, the sediment concentrations during the onset of the next flow would be dependent on the recovery period (i.e. the period between flow events). Longer recovery periods would provide a longer period of time in which fine hillslope sediment may accumulate through sediment restocking processes (e.g. Aeolian processes, bioturbation, soil freezing and thawing leading to bank collapse, bank sapping, dry ravel), which would produce higher sediment concentrations during the ensuing flow event. If the recovery period was not long enough to replace the mass of sediment evacuated during the last flow event, the next flow event would contain lower sediment concentrations than the previous flow (holding other influencing factors constant).

The effect of recovery period may explain why the fine sediment concentration displayed a slight tendency to peak at the beginning of the monsoon season and decline thereafter (as illustrated in Figure 9). During a monsoon season, flow events often occur in quick succession and have relatively short recovery periods. After the season begins, the recovery periods may not be long enough to fully restock the sediment evacuated during the previous flow event, which produces a net decrease in the entrainable fine sediment. This trend may be further promoted by the seasonal increase in vegetation density in response to the monsoonal precipitation. The increased vegetation may restrict hillslope sediment delivery to the channel system in overland flow by enhancing surficial roughness (Walling and Webb, 1982; Cotton *et al.*, 2006; Lecce *et al.*, 2006).

Figure 14 illustrates that the concentration of the fine grain-size fraction measured at the beginning of each flow event was generally greater after longer recovery periods. However, this trend displays a wide array of scatter and is not statistically significant. In a study reported by Alexandrov *et al.* (2003), the relationship between the total suspended sediment concentration and recovery period was examined in a low-ordered, ephemeral watershed in the Negev desert, Israel and no observable trend between the variables was found. The full range of environmental processes that affect sediment restocking or production rates at the relatively short-time scales analyzed in this study (i.e. flow event, seasonal, annual) are poorly understood and require further study.

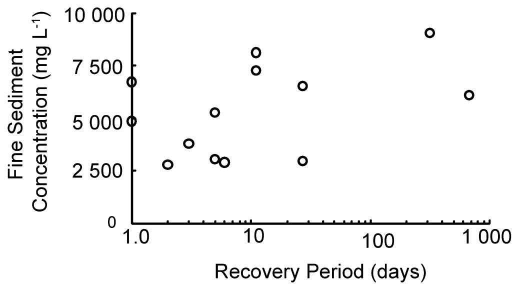

Figure 14. Fine sediment concentration (<0·25 mm) from the first sample collected during each flow event (2005–2007) plotted against recovery period.

Patterns of the coarse grain-size fraction

In contrast to the fine grain-size sediment concentration, the coarse fraction did not systematically exhibit temporal trends. There was a statistically significant negative trend between the coarse sediment concentration and flow discharge. However, the mass flux of the coarse sediment displayed a positive power-law relationship with metrics of flow strength (i.e. τ^*, τ). A large number of existing bedload transport models (e.g. Meyer-Peter and Muller, 1948; Ashida and Michiue, 1972; Fernadez Luque and van Beek, 1976) assume an exponent value near 1·5 for the power-law relationship between sediment flux and flow strength when the flow strength is much greater than that required for initial grain entrainment (i.e. $\tau^* \gg \tau^*_c$) (Garcia, 2008). That value is within the range derived for the flux of the coarse grain sizes examined in this study. The relatively high exponents computed for the power laws derived for grain sizes 0·25–1·0 mm are likely a result of the fact their observed transport values include grains traveling as bedload and in suspension.

The declining concentration of the coarse sediment in flow may have been due to sediment dilution. Because Lucky Hills is a small headwater watershed, the ratio of the volume of water entering a channel reach from overland flow and that flowing from the channel upstream is relatively large (Leopold *et al.*, 1964). Overland flow produces a net inflow of water absent of coarse sediment into the channel network because it lacks the competence to entrain and transport coarse grains. Figure 15 demonstrates the general dilution effect. As the water discharge increased at the watershed outlet, its mass typically increased at a rate greater than that of the coarse sediment in transport (the power-law exponent is less than 1·0), which decreases the sediment concentration in terms of mass. It should be noted that discharge appears on both the *x*-axis and the *y*-axis (in the sediment flux calculation) in Figure 15, creating a spurious correlation between the two represented variables.

Study results show that as the flow discharge increased, the percentage of the sediment concentration composed of the coarse grain-size fraction decreased. This was likely influenced by the decline in the concentration of the coarse grain-size fraction rather than by an increase in fine sediment because the concentration of the fine fraction was not correlated to flow discharge. Results also show that when relatively high total sediment concentrations did occur, it was primarily due to an increase in the coarse fraction. This observation is similar to that reported by Lekach and Schick (1982) in a low-ordered desert stream. They found that at above a threshold, suspended sediment concentrations increased primarily due to increases in the concentration of the coarser sediment frac-

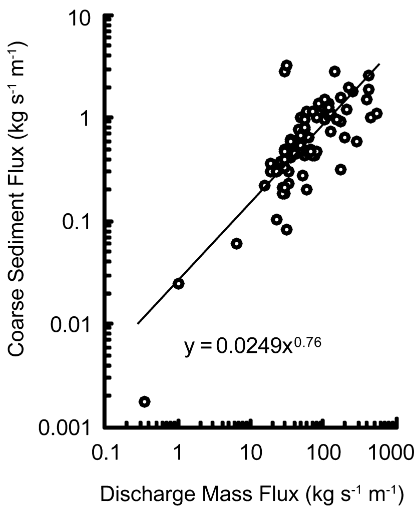

Figure 15. The calculated mass flux of the coarse grain-size fraction plotted against the mass flux of the flow discharge.

tion supplied by the channel bed. They hypothesized that the threshold was set by the maximum rate in which the hillslopes can supply wash load to the channel system, a rate dependent on the recovery period between flow events.

The decline in the coarse sediment concentration with increased discharge may have been perpetuated by instrument error if the sampler was unable to sample coarse grains with the same efficiency during high discharges as lower discharges. Instrument calibration test results (Renard *et al.*, 1986) did not explicitly report the sampling efficiency by grain size. However, the calculated coarse sediment flux values appear approximate to those reported in field studies of sediment transport in similar environments (e.g. Powell *et al.*, 1996; Malmon *et al.*, 2004) indicating these results are not anomalous.

The effect of grain-size dependent transport patterns on sediment delivery

Because of the tendency of the concentration of the fine sediment fraction to decrease with flow duration, the majority of fine sediment delivery commonly occurred during the rising limb of the hydrograph. While the concentration of the coarse grain-size fraction showed no temporal trend, the majority of the coarse sediment was delivered during the falling limb. The falling limb was usually much longer in duration than the rising limb, producing a longer period in which the coarse grains were transported by flow. Most hydrographs were singled peak, so the majority of the fine sediment yield occurred during the first half of the flow duration and the majority of the coarse grain sediment yield occurred during the second half. These phenomena underscore the importance of measuring sediment transport throughout the duration of an ephemeral flow event. This is of particular importance to sedimentation studies that require knowledge of the GSD of the mobile sediment. The results of this study show that the GSD and the relative ratio of the fine and coarse grain-size fractions often change throughout the duration of a flow event. Because of the different transport patterns based on grain size, attempts to link total sediment discharge to a single independent variable when a large distribution of grain sizes are in transport may lead to erroneous results.

Conclusions

Analysis of sediment concentrations sampled within an ephemeral, low-ordered watershed found the presence of grain-size selective transport patterns. The concentrations of sediment comprising two grain-size fractions (i.e. a fine grain-size fraction including grain sizes less than 0·25 mm and a coarser grain-size fraction including grains between 0·25 and approximately 8·0 mm) were well correlated with the concentration of the other grain sizes comprising the same fraction and less well correlated with the concentration of the grain sizes comprising the other fraction. The concentration of the coarser grain sizes were better correlated with the total sediment concentration than the concentration of the finer grain sizes. The concentration of the fine grain-size fraction, which was likely supplied from hillslope sources as wash load, decreased with flow duration and showed a slight tendency to decrease seasonally. The concentration of the coarse grain-size fraction, which was composed primarily of bed material, displayed a negative trend with flow discharge that was likely a result of dilution. The flux of the coarse sediment displayed a positive power-law relationship similar to that observed in other fluvial systems. The result of these transport patterns were calculated to play a significant role in the watershed sediment delivery; the majority of the fine grain-size sediment yield was commonly evacuated out of the watershed before the hydrograph peak and the majority of the coarse grain-size sediment yield was commonly evacuated out of the watershed after the hydrograph peak.

The results of this study show how flow strength and duration differentially affect the transport of the wash load and bed material in ephemeral flow. The results are significant because they document sediment transport in a unique fluvial environment characterized by the presence of a wide range of grain sizes available for transport as well as high sediment transport rates. Also, the study methodology permitted the collection of a wide range of sediment grain sizes using a single instrument.

Acknowledgements—Daniel Malmon and Nicole Gasparini contributed many great ideas to this research. The presentation and substance of this manuscript benefited from comments offered by Joel Johnson, Stuart Lane, and an anonymous reviewer.

References

Alexandrov Y, Laronne JB, Reid I. 2003. Suspended sediment concentration and its variation with water discharge in a dryland ephemeral channel, northern Negev, Israel. *Journal of Arid Environments* **53**: 73–84.

Alexandrov Y, Laronne JB, Reid I. 2006. Intra-event and interseasonal behavior of suspended sediment in flash floods of the semi-arid northern Negev, Isreal. *Geomorphology* **85**: 85–97.

Andrews ED. 2000. Bed material transport in the Virgin River, Utah. *Water Resources Research* **36**(2): 585–596.

Ashida K, Michiue M. 1972. Study on hydraulic resistance and bed-load transport rate in alluvial streams. *Transactions Japan Society of Civil Engineering* **206**: 59–69.

Batalla RJ, Martin-Vide JP. 2001. Thresholds of particle entrainment in a poorly sorted sandy gravel-bed river. *Catena* **44**: 223–243.

Church M. 2006. Bed material transport and the morphology of alluvial river channels. *Annual Review of Earth and Planetary Sciences* **34**: 325–354. DOI. 10.1146/annurev.earth.33.092203.122721

Church M, McLean DG, Wolcott JF. 1987. River bed gravels: sampling and analysis. In *Sediment Transport in Gravel Bed Rivers*, Thorne CR, Bathurst JC, Hey RD (eds). John Wiley & Sons: New York; 43–79.

Cohen H, Laronne JB. 2005. High rates of sediment transport by flashfloods in the Southern Judean Desert, Israel. *Hydrological Processes* **19**: 1687–1702.

Cotton JA, Wharton G, Bass JAB, Heppell CM, Wotton RS. 2006. The effects of seasonal changes to the in-stream vegetation cover on patterns of flow and accumulation of sediment. *Geomorphology* **77**: 320–334.

Dietrich WE. 1982. Settling velocities for natural particles. *Water Resources Research* **18**: 1615–1626.

Dunkerley D, Brown K. 1999. Flow behavior, suspended sediment transport and transmission losses in a small (sub-bank-full) flow event in an Australian desert stream. *Hydrological Processes* **13**: 1577–1588.

Fernadez Luque R, van Beek R. 1976. Erosion and transport of bed sediment. *Journal of Hydraulic Research. IAHR* **14**(2): 127–144.

Folk RL, Ward WC. 1957. Brazos River Bar: a study in the significance of grain size parameters. *Journal of Sedimentary Petrology* **27**(1): 3–26.

Frostick LE, Reid I, Layman JT. 1983. Changing size distribution of suspended sediment in arid-zone flash floods. *Special Publication of the International Association of Sedimentologists* **6**: 97–106.

Garcia MH. 2008. Sediment transport and morphodynamics. In *Sedimentation Engineering: Processes, Management, Modeling, and Practice*, Garcia MH (ed.). American Society of Civil Engineers: Reston, VA; 21–163.

Habersack HM, Laronne JB. 2001. Bed load texture in an alpine gravel bed river. *Water Resources Research* **37**: 3359–3370.

Hey RD. 1979. Flow resistance in gravel-bed rivers. *Journal of Hydraulic Engineering* **105**(HY4): 365–379.

Julien PY. 1998. *Erosion and Sedimentation*. Cambridge University Press: Cambridge; 280 pp.

Komar PD. 1980. Modes of sediment transport in channelized water flows with ramifications to the erosion of the Martian outflow channels. *Icarus* **42**: 317–329.

Komar PD. 1987. Selective grain entrainment by a current from a bed of mixed sizes: a reanalysis. *Journal of Sedimentary Research* **57**: 203–211.

Laronne JB, Reid I, Frostick LE, Yitshak Y. 1994. The non-layering of gravel streambeds under ephemeral flood regimes. *Journal of Hydrology* **159**: 353–363.

Lecce SA, Pease PP, Gares PA, Wang J. 2006. Seasonal controls on sediment delivery in a small coastal plain watershed, North Carolina, USA. *Geomorphology* **73**(3–4): 246–260.

Lekach J, Schick AP. 1982. Suspended sediment in desert floods in small catchments. *Israel Journal of Earth Sciences* **31**(2–4): 144–156.

Leopold LB. 1992. The sediment size that determines channel morphology. In *Dynamics of Gravel Bed Rivers*, Billi B, Hey RD, Thorne CR, Tacconi P (eds). John Wiley & Sons: New York; 297–312.

Leopold LB, Wolman MG, Miller JP. 1964. *Fluvial Processes in Geomorphology*. W. H. Freeman: San Francisco, CA.

Lisle TE. 1995. Particle size variations between bed load and bed material in natural gravel bed channels. *Water Resources Research* **31**: 1107–1118.

Malmon DV, Reneau SL, Dunne T. 2004. Sediment sorting and transport by flash floods. *Journal of Geophysical Research – Earth Surface* **109**. 13 pp. DOI. 10.1029/2003JF000067

Malmon DV, Lyman J, Reneau SL, Katzman D, Lavine A. 2007. Suspended sediment transport in an ephemeral stream following wildfire. *Journal of Geophysical Research – Earth Surface* **112**. 16 pp. DOI. 10.1029/2005JF000459

Meirovich L, Laronne JB, Reid I. 1998. The variation of water-surface slope and its significance for bed load transport during floods in gravel-bed streams. *Journal of Hydraulic Research* **36**(2): 147–157.

Meyer-Peter E, Muller R. 1948. Formulas for bed load transport. *Proceedings of the 2nd meeting, The International Association of Hydro-Environment Engineering and Research (IAHR)*, Stockholm; 39–64.

Milliman JD, Meade RH. 1983. World-wide delivery of river sediment to the oceans. *Journal of Geology* **91**: 1–21.

Morris GL, Annadale G, Hotchkiss R. 2008. Reservoir sedimentation. In *Sedimentation Engineering: Processes, Management, Modeling, and Practice*, Garcia MH (ed.). American Society of Civil Engineers: Reston, VA; 579–612.

Mudd SM. 2006. Investigation of the hydrodynamics of flash floods in ephemeral channels: scaling analysis and simulation using a shock-capturing flow model incorporating the effects of transmission losses. *Journal of Hydrology* **324**(1–4): 65–79.

Nearing MA, Nichols MH, Stone JJ, Renard KG, Simanton JR. 2007. Sediment yields from unit-source semiarid watersheds at Walnut Gulch. *Water Resources Research* **43**(6): 10 pp. DOI. 10.1029/2006WR005692

Nichols MH, Renard KG, Osborn HB. 2002. Precipitation changes from 1956–1996 on the Walnut Gulch Experimental Watershed. *Journal of the American Water Resources Association* **38**: 161–172.

Nichols MH, Stone JJ, Nearing MA. 2008. Sediment database, Walnut Gulch Experimental Watershed, Arizona, United States. *Water Resources Research* **44**(W05S06): 5 pp. DOI. 10.1029/2006WR005682

Novotny V. 1980. Delivery of suspended sediment and pollutants from nonpoint sources during overland flow. *Water Resources Bulletin* **16**: 1057–1065.

Parker G. 1990. Surface-based bed load transport relation for gravel rivers. *Journal of Hydraulic Research* **28**(4): 417–436.

Porterfield G. 1972. Computation of fluvial-sediment discharge. In *Techniques of Water-resource Investigations of the United States Geological Survey*. US Geological Survey: Washington, DC; Chapter 3, 71 pp.

Powell DM, Brazier R, Parsons A, Wainwright J, Nichols M. 2007. Sediment transfer and storage in dryland headwater streams. *Geomorphology* **88**: 152–166.

Powell DM, Reid I, Laronne JB, Frostick L. 1996. Bed load as a component of sediment yield from a semiarid watershed of the northern Negev. In *Erosion and Sediment Yield: Global and Regional Perspectives*. Proceedings of the Exeter Symposium, IAHS **236**: 389–397.

Powell MD, Reid I, Laronne JB. 2001. Evolution of bed load grain-size distribution with increasing flow strength and the effect of flow duration on the caliber of bed load sediment yield in ephemeral gravel bed rivers. *Water Resources Research* **3B7**: 1463–1474.

Raudkivi AJ. 1998. *Loose Boundary Hydraulics*. Balkema: Rotterdam; 488 pp.

Reid I, Frostick LE. 1987. Flow dynamics and suspended sediment properties in arid zone flash floods. *Hydrological Processes* **1**(3): 239–253.

Renard KG, Laursen EM. 1975. Dynamic behavior model of ephemeral stream. *Journal of the Hydraulics Division, ASCE* **92**: 511–528.

Renard KG, Simanton JR, Fancher CE. 1986. Small watershed automatic water quality sampler. *Proceedings of the 4th Federal Interagency Sedimentation Conference*, Las Vegas, NV; Vol. 1, 51–58.

Renard KG, Nichols MH, Woolhiser DA, Osborn HB. 2008. A brief background on the US Department of Agriculture Agricultural Research Service Walnut Gulch Experimental Watershed. *Water Resources Research* **44**(W05S02): 11 pp. DOI. 10.1029/2006WR005691

Shields Jr FD, Copeland RR, Klingeman PC, Doyle MW, Simon A. 2008. Stream restoration. In *Sedimentation Engineering: Processes, Management, Modeling, and Practice*, Garcia MH (ed.). American Society of Civil Engineers: Reston, VA; 461–504.

Smith RE, Chery DL, Renard KG, Gwinn WR.1981. Supercritical flow flumes for measuring sediment laden flow. *USDA-ARS Technical Bulletin* **1655**: 72.

Stone PM, Walling DE. 1997. Particle size selectivity considerations in suspended sediment budget investigations. *Water Air and Soil Pollution* **99**(1–4): 63–70.

Syvitski JP, Morehead MD, Bahr DB, Mulder T. 2000. Estimating fluvial sediment transport: the rating parameters. *Water Resources Research* **36**(9): 2747–2760.

Thorne CR, Zevenbergen LW. 1985. Estimating mean velocity in mountain rivers. *Journal of Hydraulic Engineering* **111**(4): 612–624.

Tucker GE, Arnold L, Bras RL, Flores H, Istanbulluoglu E, Solyom P. 2006. Headwater channel dynamics in semiarid rangelands, Colorado high plains, USA. *GSA Bulletin* **118**: 959–974. DOI. 10.1130/B25928.1

Walling DE, Webb BW. 1982. Sediment availability and the prediction of storm-period sediment yields. In *Recent Developments in the Explanation and Prediction of Erosion and Sediment Yield*. IAHS Publication no. 137. IAHS: Wallingford.
Walling DE, Moorehead PW. 1987. Spatial and temporal variation of the particle-size characteristics of fluvial suspended sediment. *Geografiska Annaler Series A –Physical Geography* **69**(1): 47–59.
Wentworth CK. 1926. Methods of mechanic analysis for sediments. *University of Iowa Studies in Natural History* **II**: 3–52.
Wilcock PR, McArdell BW. 1993. Surface-based fractional transport rates: mobilization thresholds and partial transport of a sand-gravel sediment. *Water Resources Research* **29**: 1297–1312.
Wood PA. 1977. Controls of variation in suspended sediment concentrations in the River Rother, West Sussex, England. *Sedimentology* **24**: 437–445.
Yuill BT, Nichols MH, Yager E. 2010. Coarse bed material patch evolution in low-order, ephemeral channels. *Catena*. **81**: 126–136 DOI. 10.1016/j.catena.2010.02.00

